

The feasibility of compensation for the azimuthal anisotropy of PS-converted waves in HTI media

Weining Liu, Hengchang Dai, and Xiang-Yang Li, British Geological Survey,

This paper studies the influence of shear-wave splitting on the azimuthal behaviour of PS converted waves in HTI media. Theoretical analysis and synthetic study show that it is more accurate to separate the fast P-SV1 component from the slow P-SV2 component before compensating for azimuthal anisotropy, especially in water-saturated fractures. NMO corrections to the P-SV1 component in dry and water-saturated models can be improved by the application of the velocity ellipse.

Introduction

Fracture detection and characterisation are important in oil and gas exploration. Vertically oriented fractures are often regarded as transverse isotropy with a horizontal symmetry axis (HTI). Thus the azimuthal anisotropy can be compensated for, to improve imaging and benefit fracture prediction.

PS converted-wave seismic data has been widely used to characterise fractured reservoirs in recent years. Current studies usually focus on compensation for the azimuthal anisotropy of PS-converted waves in the radial component (Bakulin et al., 2000; Qian et al., 2007; Dai et al., 2011). In this study, we discuss the feasibility of compensation for azimuthal anisotropy of PS converted waves in dry and water-saturated fractures. Theoretical analysis suggests that the azimuthal anisotropy of the split P-SV1 wave and P-SV2 wave is determined by the azimuthal anisotropy of both the P-wave leg and the split shear wave leg (qS1 and qS2). A synthetic study shows that separation of the P-SV1 wave and P-SV2 wave is necessary before doing other processing, especially for water-saturated fractures. Then azimuthal compensation can be applied to improve the NMO correction.

Theory

In HTI media induced by vertical fractures, the upgoing shear-wave leg of the PS converted wave instantaneously splits into a fast and slow shear-wave leg. The fast shear-wave leg is polarised in the fracture direction and the slow shear-wave leg is polarised in the direction perpendicular to the fracture direction. Consequently, both the fast (P-SV1) and slow (P-SV2) converted waves can be observed on the radial and transverse components.

In order to analyse the azimuthal variation of PS converted waves, it is necessary to understand the azimuthal behaviour of pure-mode waves. Tsvankin (1997) has proposed that the NMO velocities of pure-mode waves (P-, fast S1-, slow S2-waves) vary with azimuth and can be written as ellipses in the horizontal plane. The azimuthal variation of slow shear-wave (S2) is complicated and not considered in this study.

Liu et al (2011) simplified the elliptical equation into a cosine equation (equation (1)). Here θ is the azimuth angle, and v_{2-0° and v_{2-90° are the NMO velocities along the directions parallel and perpendicular to the fracture direction, respectively (Figure 1). Based on this, the NMO velocity of the PS converted wave can be approximated into a similar cosine function (equation (4)). Here γ_0 is the vertical velocity ratio of the P-wave to S-wave.

$$v_2^2(\theta) \approx v^2 + \Delta \cos 2\theta \quad (1) \qquad v_{ps2}^2(\theta) \approx v_{ps}^2 + \Delta_{ps} \cos 2\theta \quad (4)$$

$$v^2(v_p^2, v_{s1}^2, v_{s2}^2) = (v_{2-0^\circ}^2 + v_{2-90^\circ}^2) / 2 \quad (2) \qquad v_{ps}^2 = \left(\frac{1}{1+\gamma_0} v_p^2 + \frac{\gamma_0}{1+\gamma_0} v_s^2 \right) \quad (5)$$

$$\Delta(\Delta_p, \Delta_{s1}, \Delta_{s2}) = (v_{2-0^\circ}^2 - v_{2-90^\circ}^2) / 2 \quad (3) \qquad \Delta_{ps} = \left(\frac{1}{1+\gamma_0} \Delta_p + \frac{\gamma_0}{1+\gamma_0} \Delta_s \right) \quad (6)$$

It can be noticed from Figure 1 that for the NMO velocity ellipse of the P wave, the major axis corresponds to the fracture direction and the minor axis corresponds to the fracture normal direction. Δ_p is positive according to equation (3). The fast S1-wave follows a similar variation. So the term Δ_{s1} is also positive.

For the fast P-SV1 converted waves, Δ_{ps} is a combination of Δ_p and Δ_{s1} as equation (6) illustrates.

Δ_p and Δ_{S1} , which are positive, are combined to form the Δ_{ps} . Therefore the term is positive according to equation (6). This means that the P-SV1 wave follows a similar elliptical variation to the P-wave (Figure 2). That is why the azimuthal compensation developed for P-wave seismic data sometimes is directly used in the processing of PS converted wave data.

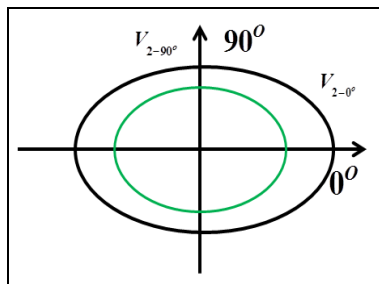


Figure 1

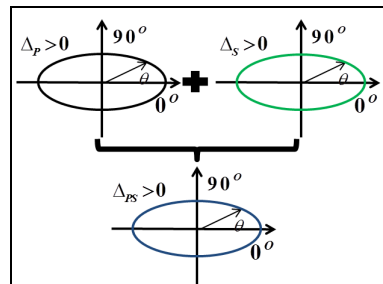


Figure 2

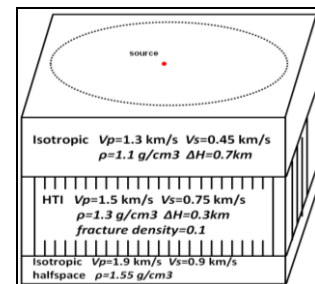


Figure 3

Figure 1: Velocity ellipses of P-wave (black), S1-wave (green). The fracture direction is 0° .

Figure 2: Velocity ellipse of P-SV1 wave (blue) is determined by velocity ellipses of P-wave (black) and S1-wave (green).

Figure 3: Model parameters (fracture direction is 120°).

Synthetic Study

A HTI layer induced by vertical fractures is created based on Hudson's theory (1980). Both dry and water-saturated cases are considered for comparison. Then this HTI layer is incorporated in a three-layer model to create a synthetic dataset using the reflectivity method (Taylor, 2001). The parameters of the HTI layer and other two layers are displayed in Figure 3. The fracture direction is 120° in the horizontal plane. The azimuthal coverage for the synthetic dataset is from 0° to 360° .

The azimuth gathers of radial, transverse and vertical component data are displayed in Figures 4 (dry model) and 5 (water-saturated model). The target event affected by the HTI layer is emphasized in the red ellipse and enlarged to facilitate the analysis. It can be observed that both the fast P-SV1 wave and slow P-SV2 wave are projected into the radial and transverse components. Compared with water-saturated fractures, dry fractures result in more significant azimuthal variations for both the P-wave and PS-converted waves. In dry fractures, the azimuthal variations of the P-SV1 wave and P-SV2 wave are similar. Therefore the radial component data sometimes is treated as a single type of PS converted wave, which could efficiently deliver satisfactory results in some circumstances. However in the water-saturated model, the azimuthal variation of P-SV1 wave is complicated by the projection of the P-SV2 wave into both radial and transverse components. Therefore it is not accurate to use the radial component data to compensate for azimuthal anisotropy.

By horizontal rotation, the individual P-SV1 component can be separated from the P-SV2 component (Figure 6). Then the azimuthal variation of P-SV1 is clearly displayed, which can be accurately compensated for, or analysed to invert for fracture properties. The fast direction for the P-SV1 wave is the fracture direction (indicated by red arrows in Figure 6) and the slow direction is the direction perpendicular to the fracture direction (indicated by blue arrows in Figure 6). Azimuthal velocity analysis can be applied to the P-SV1 component by using the elliptical equation (equation 4). Figure 7 and 8 show the NMO correction at the offset of 1000m with and without the azimuthal compensation for dry and water-saturated fractures. It can be seen that the NMO correction is improved by the application of velocity ellipses.

Conclusions

Azimuthal anisotropy of PS converted waves in HTI media is complicated by the effect of shear-wave splitting. The azimuthal variations of the P-SV1 wave and P-SV2 wave are similar in dry fractures but

different in water-saturated fractures. After the separation of the P-SV1 component from the P-SV2 component, the azimuthal anisotropy can be clearly analysed and compensated for. By applying an elliptical velocity model to the P-SV1 wave, the NMO correction result can be improved.

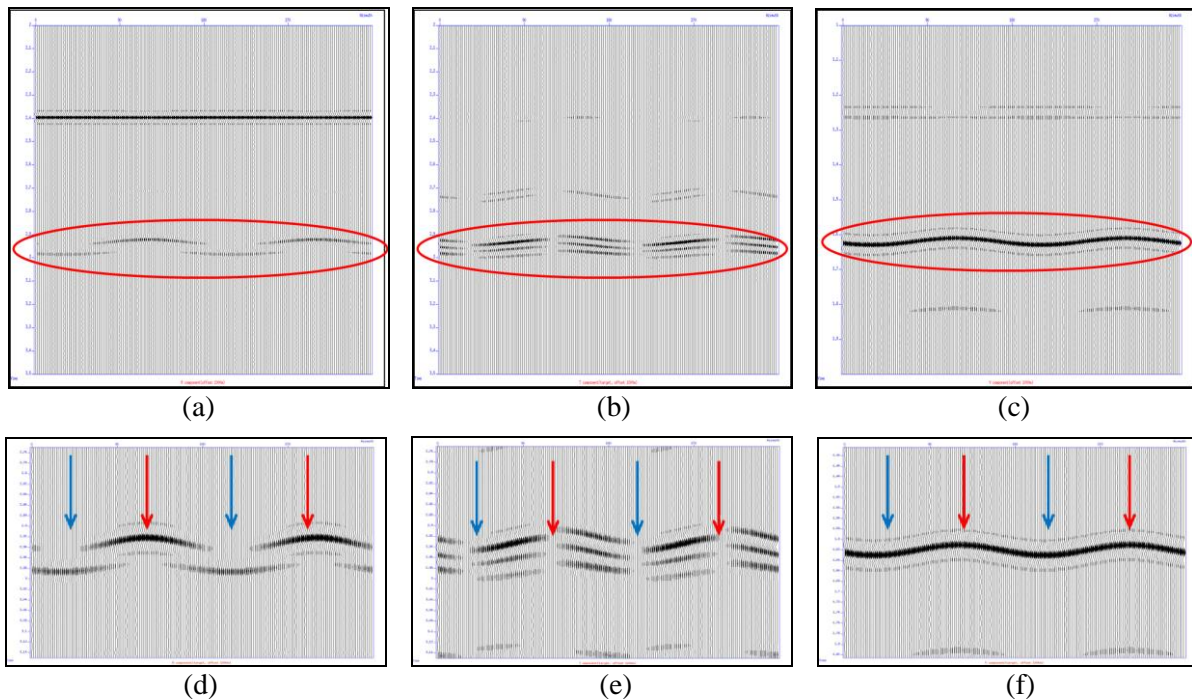


Figure 4: Azimuth gathers (offset 1000m) of radial (a), transverse (b) and vertical (c) components in the dry model. (d), (e) and (f) are enlargements of the target event emphasized by red ellipses in (a), (b) and (c), respectively. (The directions parallel and perpendicular to the fracture direction are indicated by red and blue arrows respectively).

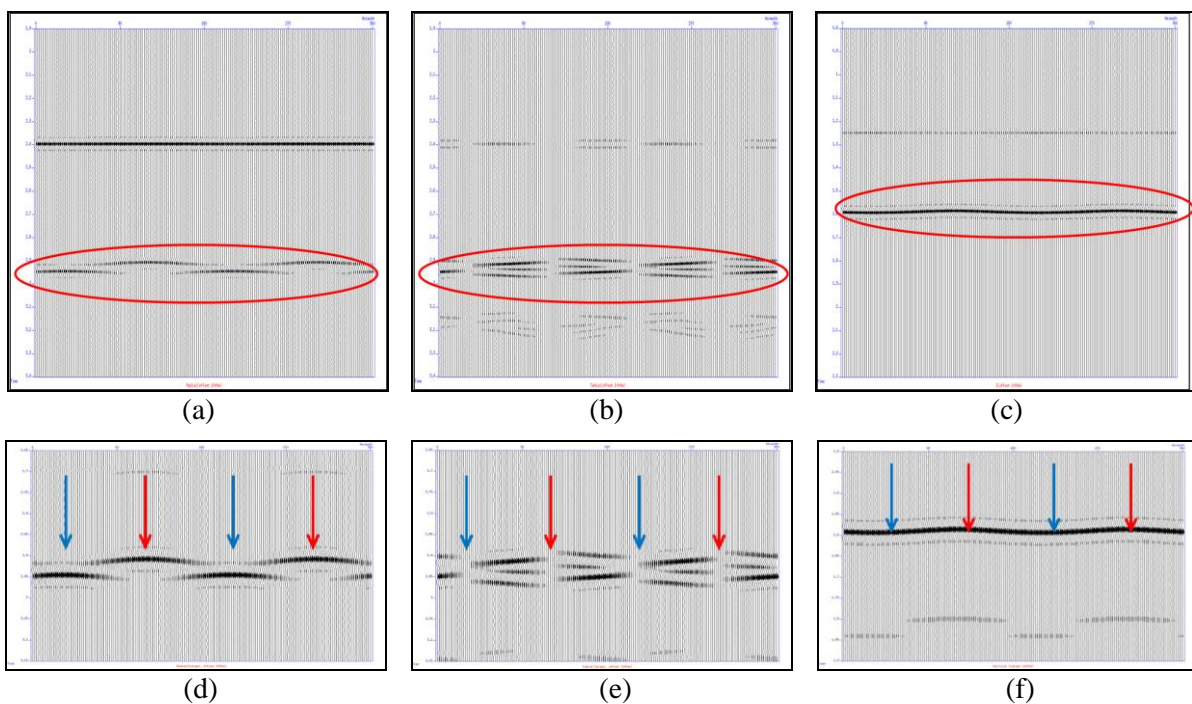


Figure 5: Azimuth gathers (offset 1000m) of radial (a), transverse (b) and vertical (c) components in the water-saturated model. (d), (e) and (f) are enlargements of the target event emphasized by red ellipses in (a), (b) and (c), respectively. (The directions parallel and perpendicular to the fracture direction are indicated by red and blue arrows respectively).

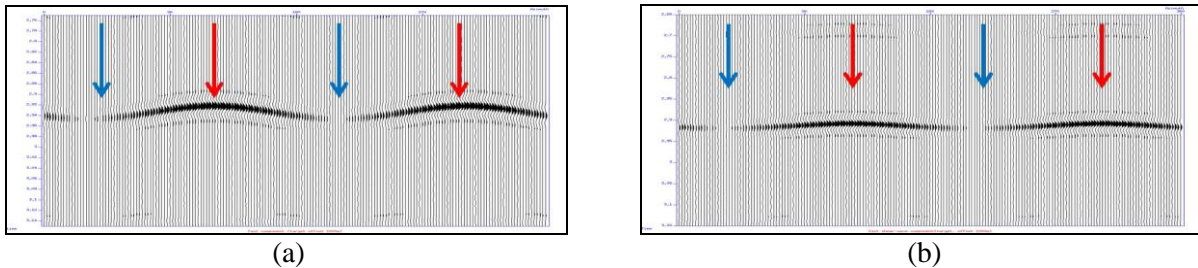


Figure 6: Azimuth gathers (offset 1000m) of the P-SV1 component in the (a) dry, and (b) water-saturated models. (The directions parallel and perpendicular to the fracture direction are indicated by red and blue arrows respectively).

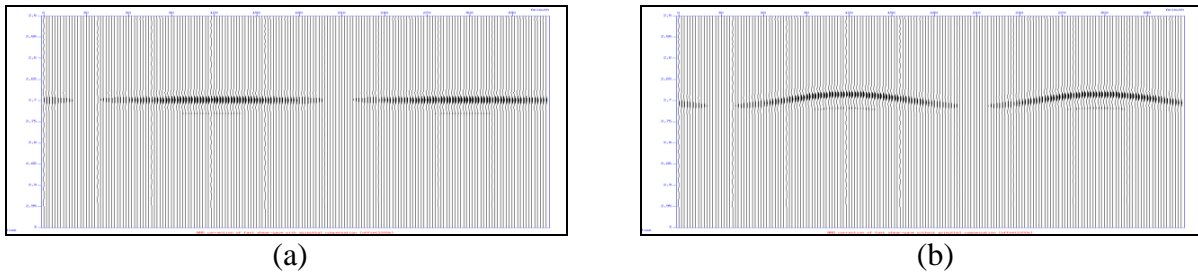


Figure 7: NMO correction results at 1000m offset for the P-SV1 wave (a) with, and (b) without the velocity ellipse in the dry fracture model.

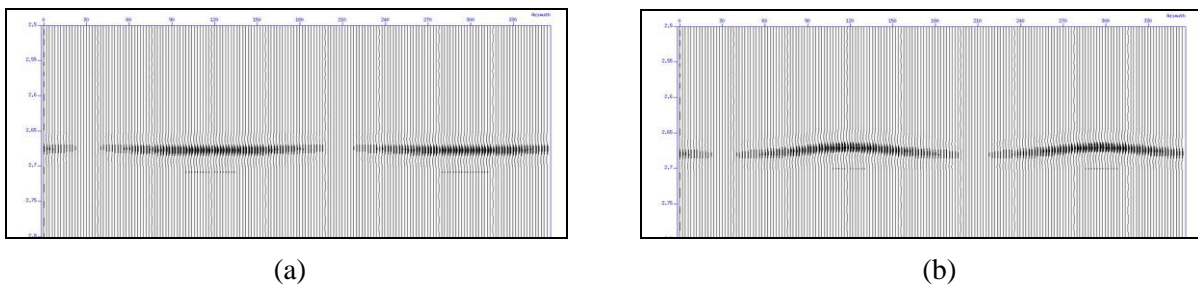


Figure 8: NMO correction results at 1000m offset for the P-SV1 wave (a) with, and (b) without the velocity ellipse in the water-saturated fracture model.

Acknowledgements

This work is supported by the Edinburgh Anisotropy Project (EAP) of the British Geological Survey, and is published with the permission of the Executive Director of the British Geological Survey (NERC) and the EAP sponsors

References

- Bakulin, A., Grechka, V. and Tsvankin, I., 2000, Estimation of fracture parameters from reflection seismic data-Part I: HTI model due to a single fracture set. *Geophysics*, **65**, 1788-1802.
- Dai, H., Li, X-Y., Ford, R., Yu, C. and Wang, J., 2011, Fracture detection using PS converted waves: A case study from Daqing Oil field, 81st SEG Annual Meeting, Expanded Abstracts, 30, 1318-1322.
- Hudson, J.A., 1980, Overall properties of cracked solid, *Math. Proc. Camb. phil. Soc.*, **88**, 371-384.
- Qian, Z., Li, X-Y., Chapman, M., 2007, Azimuthal variations of PP- and PS-wave attributes: a synthetic study, 77th SEG Annual Meeting, Expanded Abstracts, 26, 184-187.
- Taylor, D.B., 2001, *Manual: Version 5.5 Macro Ltd*, 31 Palmerston Place, Edinburgh.
- Tsvankin, I., 1997, Reflection moveout and parameter estimation for horizontal transverse isotropy, *Geophysics*, **62**, 2, 614-629.